Stimuli-responsive and chemically tunable organic microcrystal laser switch

Xin Cai [a], Zhenzhen Xu [a], Xiaolin Zheng [a], Chenhui Ran[a], Peng Liu [b], Xianxiong He [b], Xue Jin [b], Qing Liao [a] and Hongbing Fu* [a,b]*

[a]Beijing Key Laboratory for Optical Materials and Photonic Devices, Department of Chemistry, Capital Normal University, Beijing 100190, China

[b]Tianjin Key Laboratory of Molecular Optoelectronic Sciences, Department of Chemistry, Tianjin University and Collaborative Innovation Center of Chemical Science and Engineering (Tianjin), Tianjin 300072, P.R. China

*Correspondence to: xuzhenzhen@cnu.edu.cn; hbfu@cnu.edu.cn

Contents:

Experimental section

Additional data and results

Experimental Section

1. Synthesis and Compound Data

All chemicals were purchased from Beijing Innochem Agent Ltd. All chemicals were of analytical grade and used without further purification. All reactions involving air-sensitive reagents or intermediates were carried out under argon atmosphere. All solvents for extraction, and thin layer chromatography (TLC) were distilled before use. Ultrapure water with a resistance of 18.2 M Ω·cm-1, produced by using a Milli-Q apparatus (Millipore), was used in all experiments. The compound, 4,4'-((1E,1'E)-(((1E,1'E)-(2,5-dimethyl-1,4-phenylene) bis(ethene-2,1-diyl))bis (2,5-dimethoxy-4,1-phenylene))bis(ethene-2,1-diyl))bis(N,N-dimethylaniline) (OPV-DMBA) was synthesized using a classical Horner–Wadsworth–Emmons coupling reaction. ^{1}H-NMR spectra were recorded on a Varian (600 MHz) at Capital Normal University. Chemical shifts δ in ppm are referenced to the solvent residual peak ($CDCl_3$: 1H δ = 7.26) as an internal standard. Peak multiplicities are given as followed: s, singlet; d, doublet; m, multiplet. Thin layer chromatography (TLC) was carried out on silica gel GF254 plates; detection with UV light (330 - 380nm). The ground state geometries were fully optimized by the density functional theory (DFT) method with the Becke three-parameter hybrid exchange and the Lee-Yang-Parr correlation functional (B3LYP) and 6-31G** basis set using the Gaussian 03 software package.

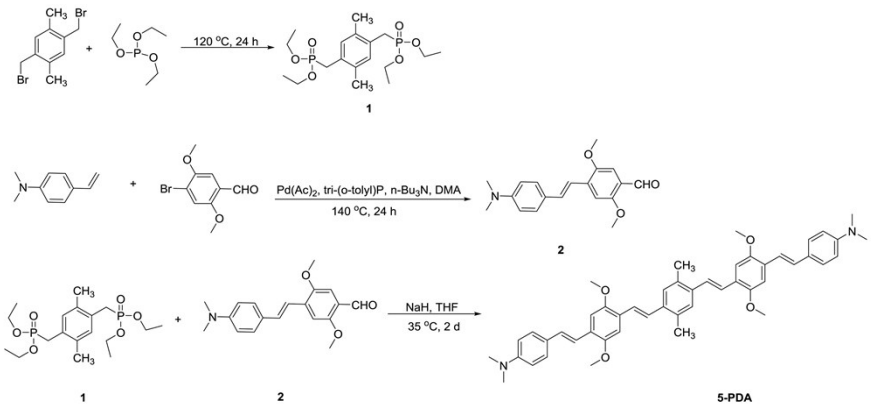

Scheme S1. The synthetic routes of 4-(4-(4-(4-(4-(dimethylamino)styryl)-2,5-dimethoxystyryl) -2,5-dimethylstyryl)-2,5-dimethoxystyryl)-N,N-dimethylbenzenamine (OPV-DMBA)

1.1 Synthesis of tetraethyl ((2,5-dimethyl-1,4-phenylene)bis(methylene))bis(phosphonate) (1)

A mixture of 1,4-bis(bromomethyl)-2,5-dimethylbenzene (0.81 g, 2.77 mmol) and triethylphosphite (1.05 mL, 6.25 mmol) was stirred at 140 °C (bath temp) for 24 h. The excess triethylphosphite was removed in vacuo under the reduced pressure. The viscous liquid was used without further purification.

MALDI-TOF: m/z calculated for [M]: 406.1; found: 406.1.

1.2 Synthesis of (E)-4-(4-(dimethylamino)styryl)-2,5-dimethoxybenzaldehyde (2)

A mixture of N,N-Dimethylacetamide (DMA) (20mL), 4-bromo-2,5-dimethoxybenzaldehyde (244 mg, 1.0 mmol), Palladium (Ⅱ) acetate (4.35 mg, 0.05 mmol), tris(2-methylphenyl)phosphine (152.0 mg, 0.5 mmol), N,N-dimethyl-4-vinylaniline(220.5 mg, 1.5 mmol) and Tri-n-butylamine (2 mL) were stirred at 140 °C for 24 h under argon atmosphere. After cooled to room temperature, HCl solution (1 M, 50 mL) was added to the solution. The mixture was extracted with EtOAc (6 × 50 mL). The combined organic phases were washed with NaCl saturated solution (50 mL), dried over Na_2SO_4, filtered, and evaporated. The product was separated by flash chromatography on silica gel by means of CH2Cl2/petroleum ether (1:20). Finally a highly fluorescent light-green powder was obtained as the title compound (0.202 g, 0.65 mmol) in 65% yield.

MALDI-TOF: m/z calculated for [M]: 311.1; found: 311.1.

1.3 Synthesis of OPV-DMBA

A mixture of THF (anhydrous, 30mL) of NaH (200 mg, 8.33 mmol), compound (2) (311 mg, 1.00 mmol) was stirred at 0 °C for 30 min under argon atmosphere. Then compound (1) (203 mg, 0.50 mmol) was added to the solution. The mixture was stirred at 0 °C for 1 h and then heated at 35 °C for 2 d. After cooled to room temperature, ultrapure water (100 mL) was added to the solution. The mixture was extracted with DCM (6 × 50 mL). The combined organic phases were washed with NaCl saturated solution (100 mL), dried over Na_2SO_4, filtered, and evaporated. The product was separated by flash chromatography on silica gel by means of (dichloromethane / ethanol = 40:1). Finally a highly fluorescent light-green powder was obtained as the title compound (0.207 g, 0.29mmol) in 58% yield.

HR-MALDI: m/z calculated for [M]: 720.3927; found: 720.3921. **^{1}H-NMR** (600 MHz, $CDCl_3$): δ (ppm): 2.45 (s, 6H, -CH_3), 2.99 (s, 12H, -NCH_3), 3.92 and 3.93(s, 12H, -OCH_3), 7.06 (d, J = 16.2

Hz, 2H, =H), 7.37 (d, *J* = 16.2 Hz, 2H, =H), 7.11-7.47 (m, 14H, Ph-H). **Elem.Anal.** C:79.91%; H:7.32%; N: 3.90%; O: 8.87%.

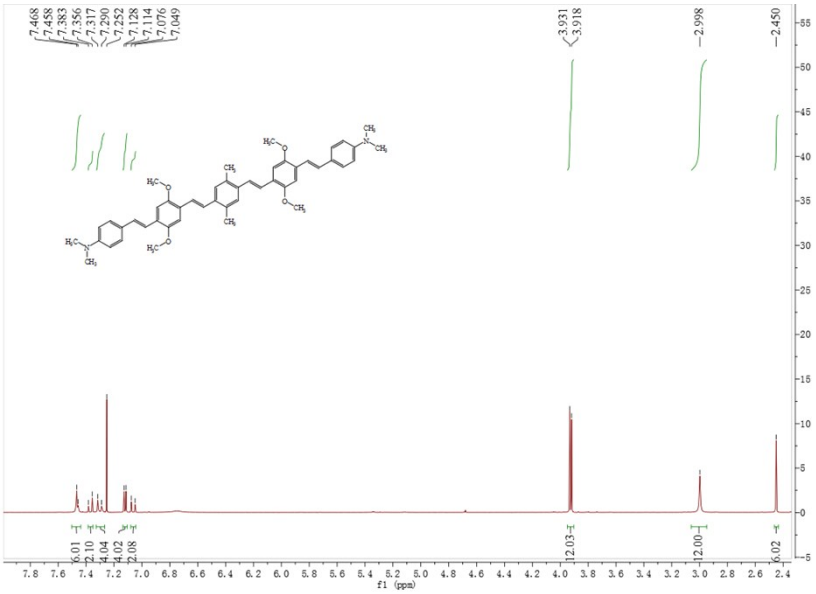

^{1}H NMR spectra of 5-PDA recorded in $CDCl_3$ (600 MHz)

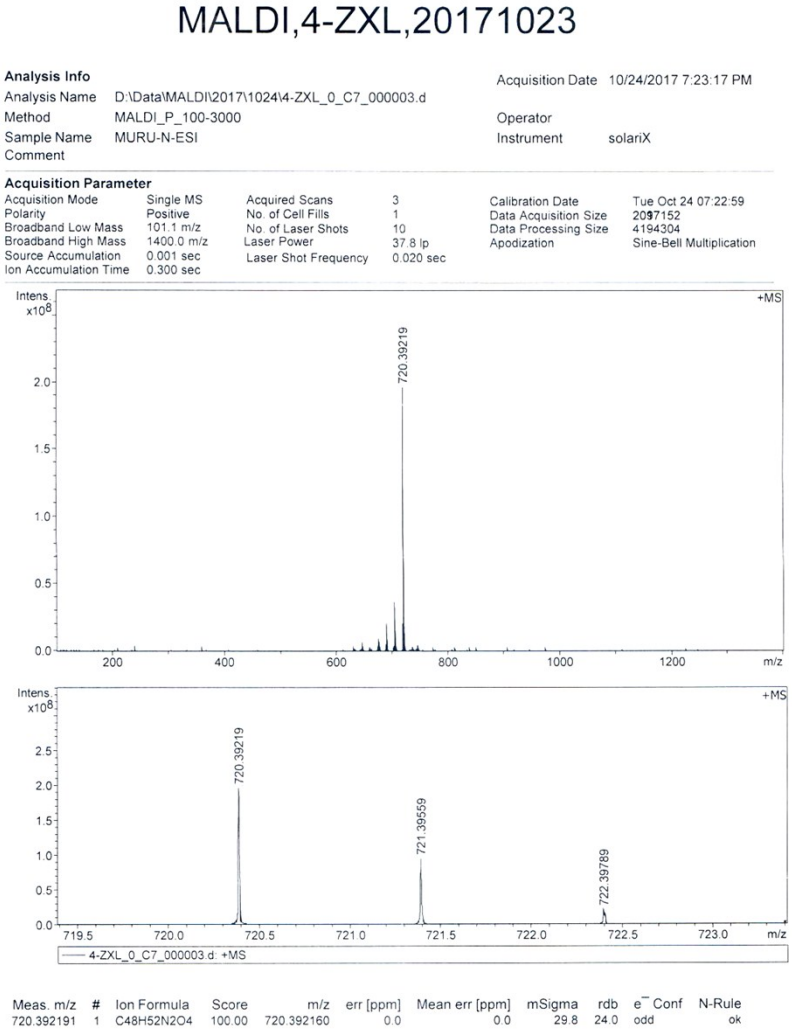

HR-MALDI spectra of OPV-DMBA

2. Preparation of OPV-DMBA **microbelts**

The OPV-DMBA microbelts (MBs) were prepared by drop-casting 200 μL of OPV-DMBA solution ($5.0 * 10^{-4}$ M in THF) on the glass substrate at room temperature. With the evaporation of the THF, the decrease of solubility together with the strong intermolecular □π-π□ interactions provide driving forces for the OPV-DMBA molecules to aggregate and self-assemble quickly into one-dimensional MBs.

3. Structural characterization

The morphologies and sizes of OPV-DMBA microbelts were examined using field emission scanning electron microscopy (FESEM, Hitachi S-8010) at acceleration voltages of 10-15 kV. Prior to analysis, the samples were coated with a thin platinum layer using an Edwards Sputter

Coater. Transmission electron microscopy (TEM) images and the selected-area electron diffraction (SAED) pattern were obtained by a JEOL JEM-2100. One drop of the as-prepared sample dispersion was deposited on a carbon-coated copper grid, and dried under high vacuum. TEM measurement was performed at room temperature at an accelerating voltage of 100 kV. X-ray diffraction patterns were measured by a D/max 2500 X-ray diffractometer with Cu Kα radiation (λ = 1.54050 Å) operated in the 2θ range from 1° to 60°.

4、Ion chromatography experiment

The OPV-DMBA microbelts (1.9 mg) were prepared by drop-casting OPV-DMBA solutionon the glass substrate at room temperature. The OPV-DMBA microbelts were placed in a culture dish and treated with 60 ppm HCl vapor for 10 minutes. The wavelength of the microlaser was swithed to 560 nm. Then, the MBs@HCl were placed in a volumetric flask. When adding H_2O (1mL) into the volumetric flask, Cl^- were dissolved in water. The wavelength of the microlaser can be swithed back to 585 nm. The Cl- in aqueous sample were tested using ion chromatography. The Cl^- in aqueous sample was 2944 ng/mL. The mole fraction of OPV- $DMBA^+ \cdot HCl^-$ in MBs@ HCl is ~0.03. Considering the thickness of the MBs is about 200 nm, and the height of one layer of DMBA molecules along the c-axis in MBs is 20.83Å. These results verify the formation of unilayer of $DMBA^+$ HCl^- on the surface of the microbelts, which belongs to chemical adsorption.

5. Optical characterization

The absorption and emission spectra were measured on Shimidazu UV-3600 UV-VIS-NIR and Horiba FluoroMax-4-NIR spectrophotometers, respectively. The relative fluorescence quantum yield Φ of the solution was measured using R6G as a reference (Φ=0.94), while the absolute fluorescence quantum yield of OPV-DMBA MBs were measured by using the integrating sphere equipped on the FluoroMax-4-NIR spectrophotometer.

PL images of ensemble microbelts placed on glass slides were recorded using an Olympus research inverted system microscope (FV1000-IX81, Tokyo, Japan) equipped with a charge couple device (CCD, Olympus DP71, Tokyo, Japan) camera. The excitation source is a Xenon lamp equipped with a band-pass filter (330~380 nm for UV-light, 460-490 nm for blue light) and the samples were deposited onto a glass slide.

The optically pumping laser measurements of OPV-DMBA microbelts were investigated at room temperature in air by a home-made optical microscopy equipped with a 50×0.9 NA

excitation objective. The samples on glass substrates of the confocal dish were transferred on the 2D movavble sample table of the optical microscope. The second harmonic (400 nm, 150 fs, 1 kHz) of a regenerative amplifier (Spitfire, Spectra Physics) seeded with a mode-locked Ti:sapphire laser (Tsunami, Spectra Physics) was focused to a 150-μm-diameter spot to excite the selected 5-PDA microbelt. The pump intensity of the pulse laser varied using a series of metallic neutral density filters. The PL spectra were collected underneath by using a 50×0.9 NA Objective that was mounted a 3D movable stage. A 430-nm long-wave pass dielectric filter was used to block any scattered excitation light. Finally the collected PL was coupled to an optical fiber and detected using a liquid-nitrogen-cooled CCD (SPEC-10-400B/LbN, Roper Scientific) attached to a polychromator (Spectropro-550i, Acton Research Corp.). The spectral resolution is 0.01 nm.

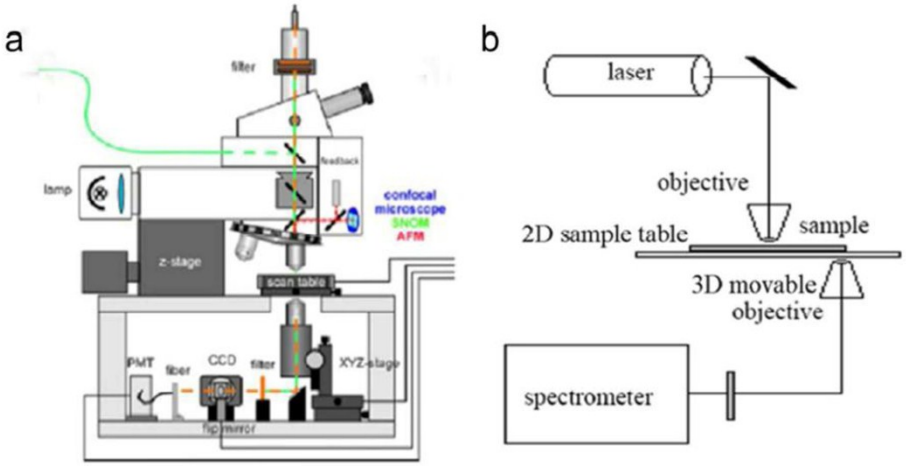

Scheme S2. Schematic illustration of the near-field scanning optical microscopy (left) and the transmittance optical path for the spatially resolved PL measurements (right).

Additional data and results

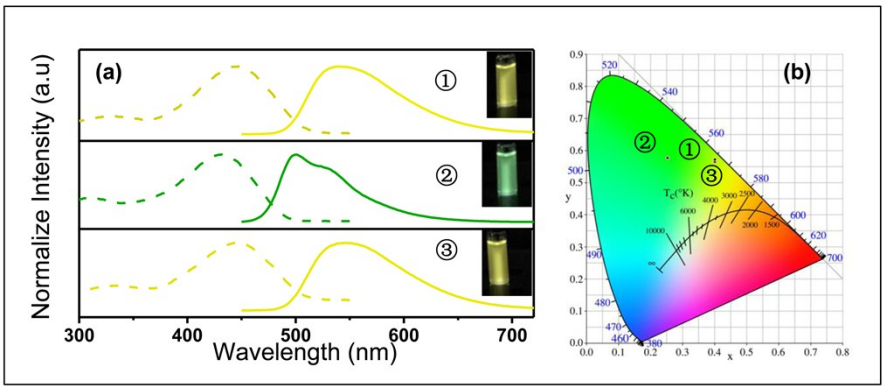

Figure S1. (1) Normalized UV−vis absorption and PL spectra of OPV-DMBA in THF solution（upper panel , adding with excess HCl (middle panel) and the adding with NH_3. The inset photographs are corresponding THF solution under UV light illumination (330–380 nm).

The dyes concentrations are all 1.0 * 10^{-5} M. (2) CIE coordinates indicating that the emission of ①, ② and ③.

- The emission spectrum of OPV-DMBA in THF solution (①) exhibits vibrionic progression bands with the maximum emission peak at 541 nm with a CIE (Commission Internationale de L'Eclairage) (CIE= 0.40, 0.57), which is in the region of yellow-green.
- Upon protonation, the emission band was hypsochromic shift to 500 nm, which exhibts a green emission (CIE 0.25, 0.58).
- When added the NH_3 solution, the solution after protonation recovered to its yellow-green emission at 541nm (CIE 0.40, 0.57).
- Moreover, the switch between yellow-green to blue-green emission can be repeated by adding the HCl and NH_3 solution, demonstrating the significant fluorescent switching properties of the OPV-DMBA solution under protonation/deprotonation stimuli.

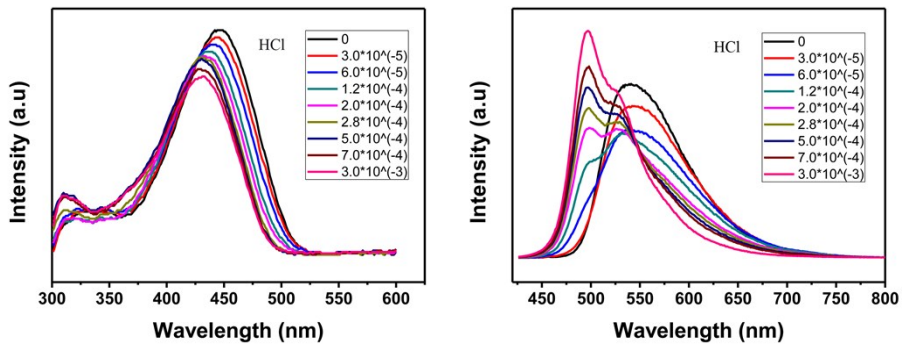

Figure S2. The evolution of the absorption and fluorescence emission spectra of OPV-DMBA (1.45×10^{-6} M) in THF upon adding HCl gradually.

- In order to explain the drastic changes unpon protonation, the evolution of the absorption and fluorescence emission spectra of OPV-DMBA (1.45×10^{-6} M) in THF upon adding HCl gradually were shown. Without HCl, the yellow solution shows an absorption band centered at 444 nm. Upon the addition of HCl, the band of 444 nm was quenched with blue-shifting to 431 nm as HCl concentration increased to 3.0×10^{-3} M. The new absorption at 431 nm can be assigned as the new $S_0 \rightarrow S_1$ induced by the enhanced electron acceptor ability of the *N,N*-

dimethylamino group upon protonation. The corresponding PL spectra unpon protonation process shows that neutral OPV-DMBA in THF solution exhibits an intense emission band centered at 541 when excited at 400 nm. Initial addition of HCl caused a distinct emission decrease in the 541nm and a sligthly increase of the bands in the 530 nm. When the concentration of the HCl reachend to 1.2×10^{-4} M , the band of the 541 nm decreases in intensity as the blue-shifted band at 500 is promoted. It is notable that we obviously observe a isosbestic point in the emission spectra: at 547 nm for the data between 2.0×10^{-4} and 3.0×10^{-3} M HCl. The isosbestic point centered at 547nm observed during the titration process implies that there might be two defined species, a neutral and a protonated one. In this case, the band in the 500 nm can be assigned as the π-π* transition in an electron-poor protonated state and the band in the 541 nm can be assigned as the π-π* transition in an electron-rich neutral states.

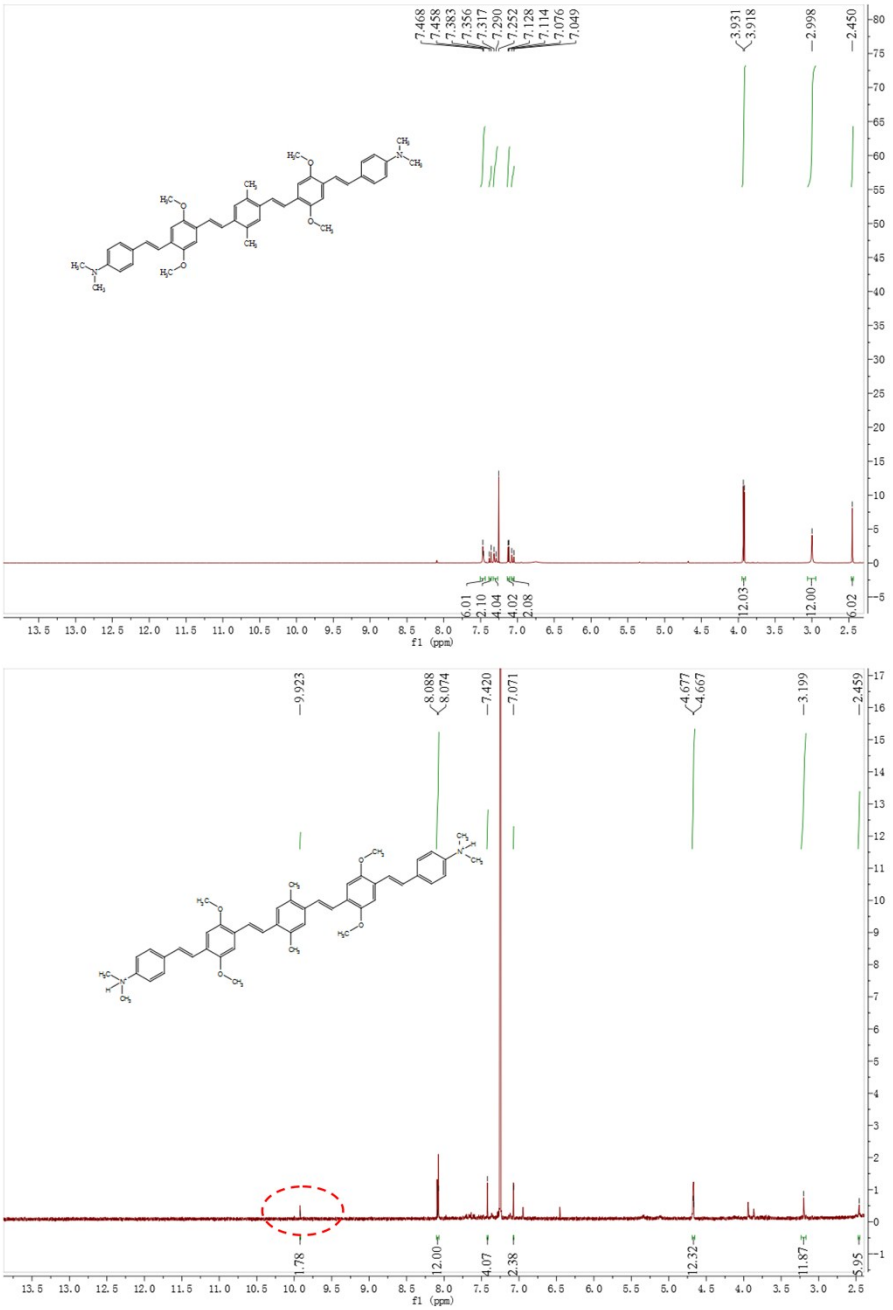

Figures S3. 1H NMR spectra of OPV-DMBA and OPV-DMBAH^{+}·Cl^{-} recorded in CDCl3 (600 MHz). The peak at 9.923 ppm can be attributed to the H in NH^{+}.

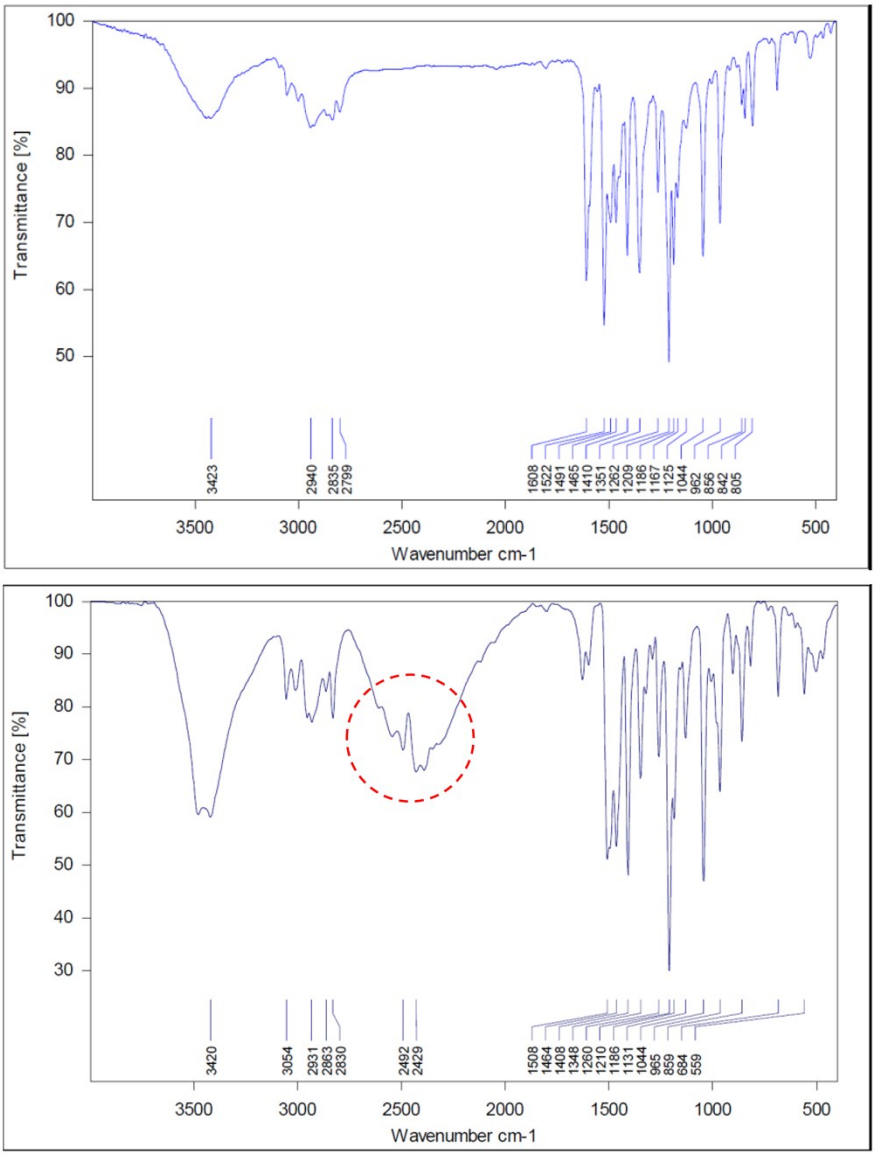

Figures S4. IR spectra of OPV-DMBA powder and OPV-DMBAH^{+}·Cl^{-} powder.

- There are peaks around 2500 cm^{-1} in spectra of OPV-DMBAH^{+}·Cl^{-} powder, which can be attributed to the N-H stretching vibration. The result show the formation of the OPV-DMBAH^{+}·Cl in powder after exposure to HCl vapor.

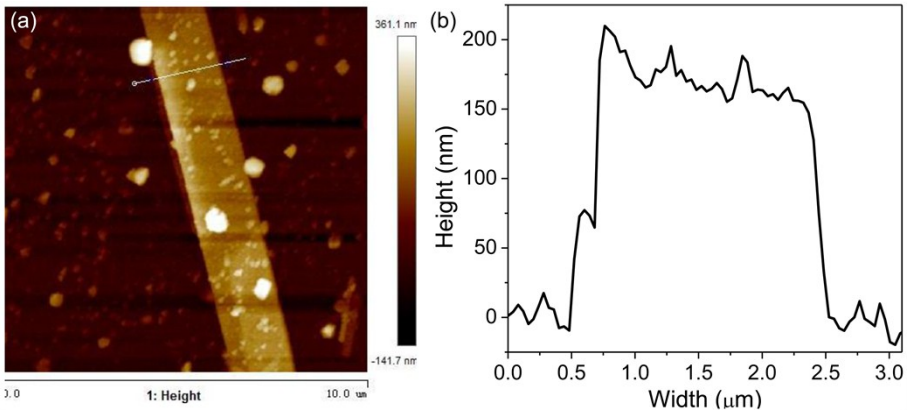

Figure S5. AFM image of individual MBs with a width of 2 μm. Right top insets: topography line profiles measured across MBs . The height is about 170 nm.

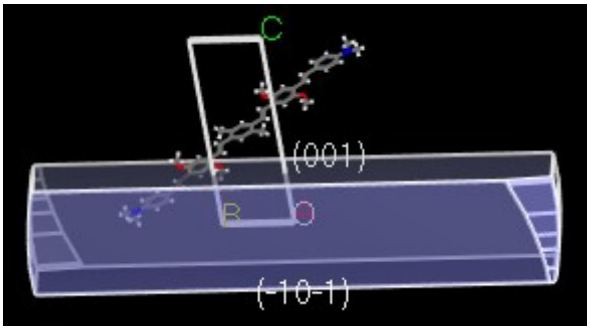

Figures S6. Equilibrium shape of OPV-DMBA for minimum total surface energy, calculated by the Materials Studio package software.

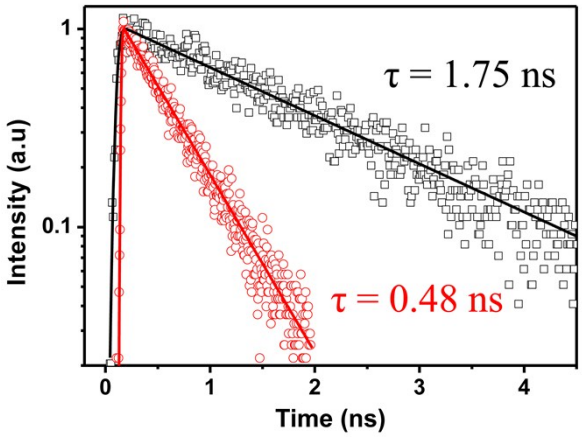

Figure S7. Fluorescence decay profiles of OPV-DMBA monomers in THF solution (τ =1.75 ns) and a single OPV-DMBA MB on a glass substrate. (τ = 0.48ns).

Table S1 Photophysical parameters of 5-PDA monomers in THF solutions and MBs on glass substrate

	λ_{abs} [a] (nm)	ε [a] ($M^{-1}cm^{-1}$)	λ_{em} (nm)	Φ	τ [b] (ns)	κ [c] (ns^{-1})
monomers	444	107200	545	0.82	1.75	0.46
MBs	401	--	585	0.10	0.48	0.21

[a] Molar extinction coefficient at the maximum absoption wavelength of λ_{abs}. [b] Fluorescence life time. [c] Radiative decay rate calculated according to $\kappa_r = \Phi/\tau$

- Compared with the monomer in THF solution, the absorption spectra of these microcrystals exhibit a strongly blue-shifted maximum around 401 nm, with additional A1 bands around 515 nm. The blue-shifts of these microcrystals suggest that the 5-PDA molecules form H-aggregates in these crystals.
- The average fluorescence lifetimes τ were estimated to be 1.75 ns for monomers and 0.48 ns for microcrystals.(Table S1). According to the equation kr = Φ_F/τ, the radiative decay rates (k_r) are calculated and shown in Table S1.
- Moreover, the fact that kr of the crystals are slower than that of the monomers is the fingerprint of H-aggregation model.

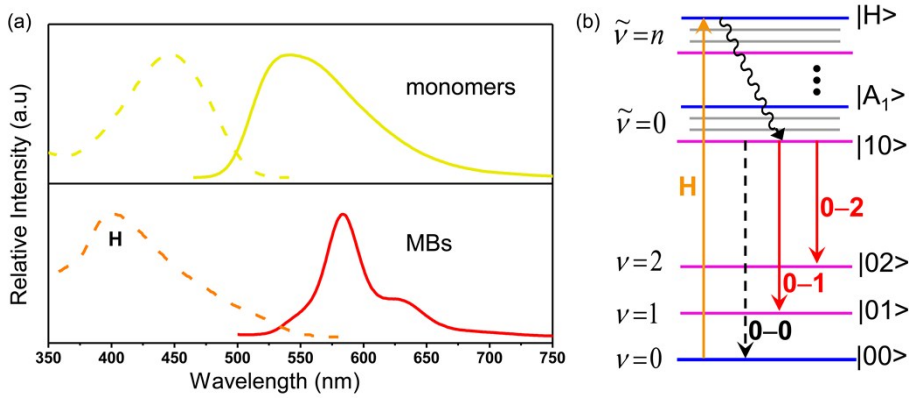

Figure S8. a) Absorption (dash) and normalized PL (solid) spectra of assembled MBs (lower) placed on a glass substrate and monomers in THF solution (upper). b) Energy level diagram for the optical transitions of OPV-DMBA MBs H-aggregates. Blue energy levels correspond to nodeless excitons accessed by photon absorption, which then vibrationally relax to the lowest energy | 10⟩ node excitons as indicated by the upper waved arrow. Because of optical rules, the | 10⟩ ↔ | 00⟩ transitions are forbidden. The weakly observed 0 − 0 emission in bottom panel of (a) is due to the presence of a low density of side disorders in single-crystalline MBs.

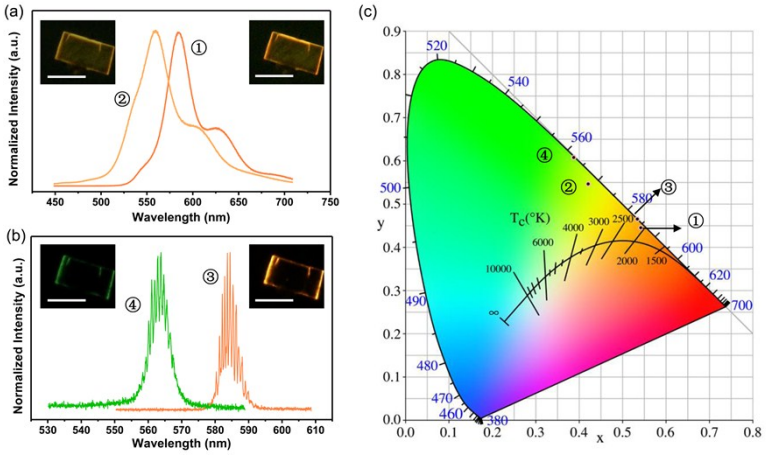

Figure S9. (a) Normalized PL spectra of a single MB ① and MB exposure to HCl vapor ② placed on a glass substrate below the threshold. Inset: The corresponding photoluminescence (PL) microscopy images of MB ① and MB ② on a glass. The scale bar is 20 μm. (b)) Normalized PL spectra of a single MB ③ and MB exposure to HCl vapor ④ placed on a glass above the threshold. Inset: The corresponding photoluminescence (PL) microscopy images of MB ③and MB ④ on a glass substrate. The scale bar is 20 μm. (c) CIE coordinates indicating that the emission of ①(CIE=0.54, 0.44),②(CIE=0.42, 0.55) , ③(CIE=0.54, 0.46).and ④(CIE=0.39, 0.61).

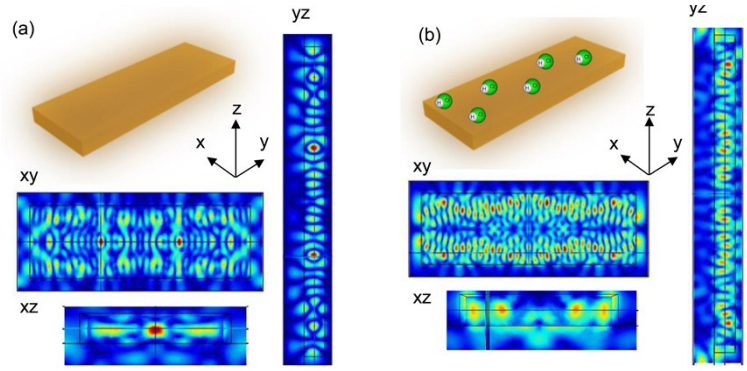

Figure S10. The scheme of the model in finite-difference time-domain (FDTD) simulations and the cross-sectional views of the mode profile that are taken at the xy, xz, yz slice of the MBs (585 nm, a) and MBs@HCl (560 nm, b) cavity.

- To identify the cavity mode within the MPs, the simulation of local electric field $|E|^2$ distribution in the microcavity was performed by using the FDTD method. The width/height and the length of the cavity are set as 2/0.3 and 6 μm. The lasing wavelength is located around 585 nm and 560 nm respectively. The refractive indexes of MBs is 1.95. The electric field distribution of the xy, xz and yz sections were simulated. The calculated result show efficient FP mode pattern in xy sections with nearly all the electric field $|E|^2$ intesities are

limited inside in the inner surface of four edges of MBs.

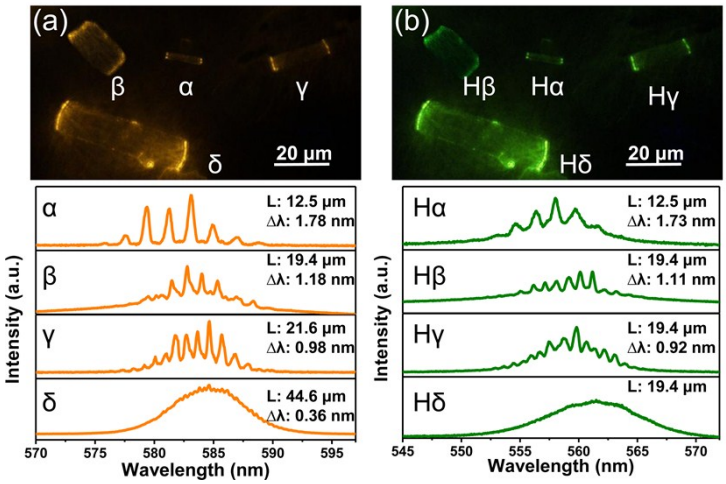

Figure S11. (a and b) Photoluminescence (PL) microscopy images of ensemble 5-PDA MBs and MBs@HCl on a glass substrate of the confocal dish excited with 400 nm, 150 fs light above the threshold. The scale bar is 20 μm. (c and d) High-resolution PL spectra of ensemble 5-PDA MBs and MBs@HCl on a glass substrate of laser emission recorded above threshold for 5-PDA microbelts with different width.

- The mode spacing Δ λ at 585 and 560 nm decreases while the length of 5-PDA microbelt increases.

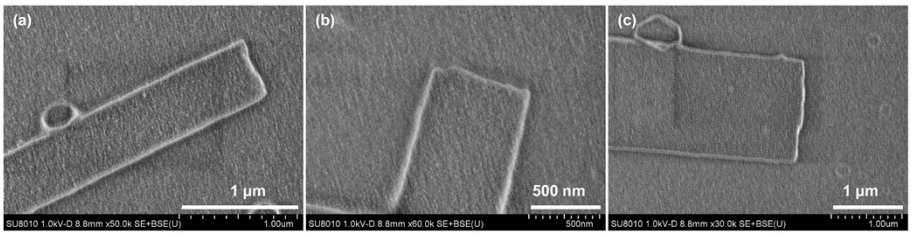

Figures S12. SEM images of a single MB (a), MB@HCl (b) and MB@HCl teated with NH_3 (c). The morphologies show no difference with the HCl-NH_3 vapor cycle.

- Moreover, under the high vacuum environment of the SEM, the HCl molecules on the surface of the belts were desorption, which is verified by the recovery of lasing peaks to 585 nm.
- Using the Gaussian03 programs at B3LYP/6-31G** level, the energy change containing zero-point vibrational energy in DMBA + HCl -> DMBA·HCl gas phase is -6.96 Kcal/mol, and the changes of Gibbs free energy is 1.97 Kcal/mol at normal temperature, which is very small. The reaction is basically reversible, which is consistence with the experiment results.

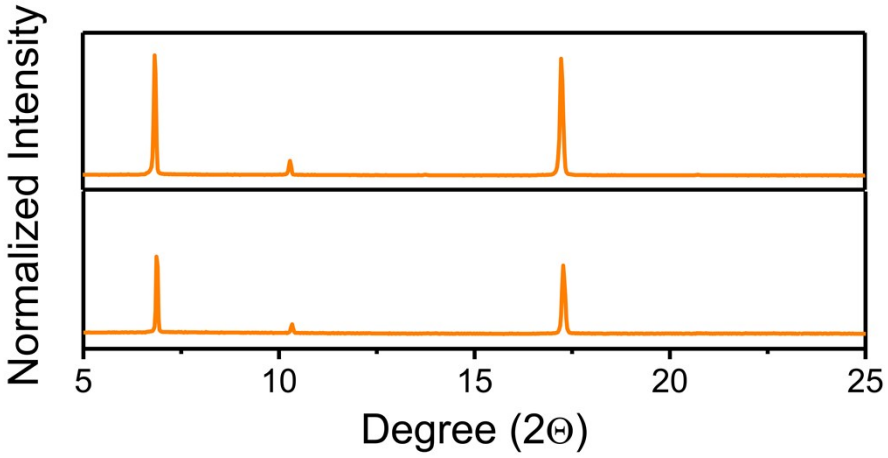

Figures S13. XRD spectra of MBs (top) and MBs @HCl.(down). The XRD peaks of the MBs@HCl can be perfectly indexed to the MBs.

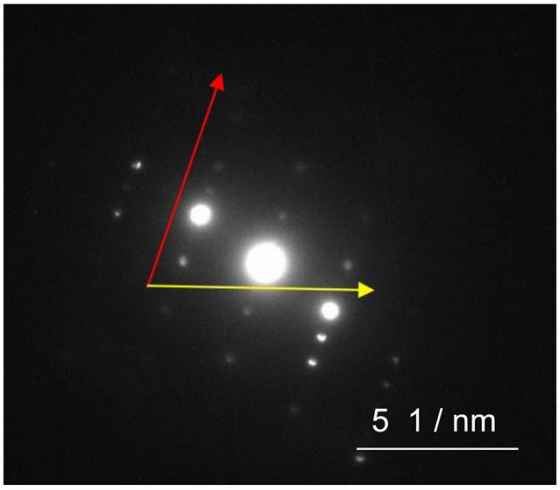

Figures S14. The SAED of a single MBs@HCl.

- The corresponding d-spacing values are 4.08 Å and 6.02 Å with the angle 78.6 º, which is same to the SAED of the MBs in Figure 2.
- Moreover, under the high vacuum environment of the TEM, the HCl molecules on the surface of the belts were desorption, which is verified by the recovery of lasing peaks to 585 nm.

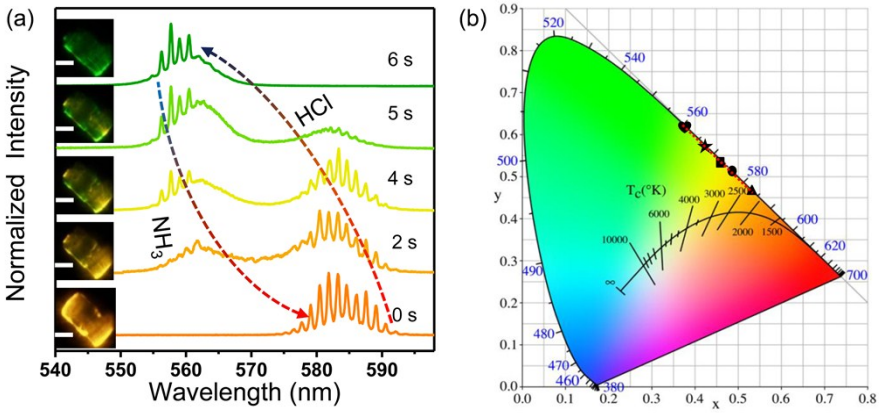

Figure S15 (a) Wavelength shift from to 585 nm to 560 nm of the microlaser with the different exposure time after adding saturated HCl solution. The insert are the corresponding optical images of the MBs@HCl at different exposure time with a scale bar of 5 μm. After adding the saturated NH_3 solution, the wavelength of the microlaser can be swithed back to 585 nm. (b) CIE coordinates indicating that the emission of microlaser with the different exposure time after adding saturated HCl solution.

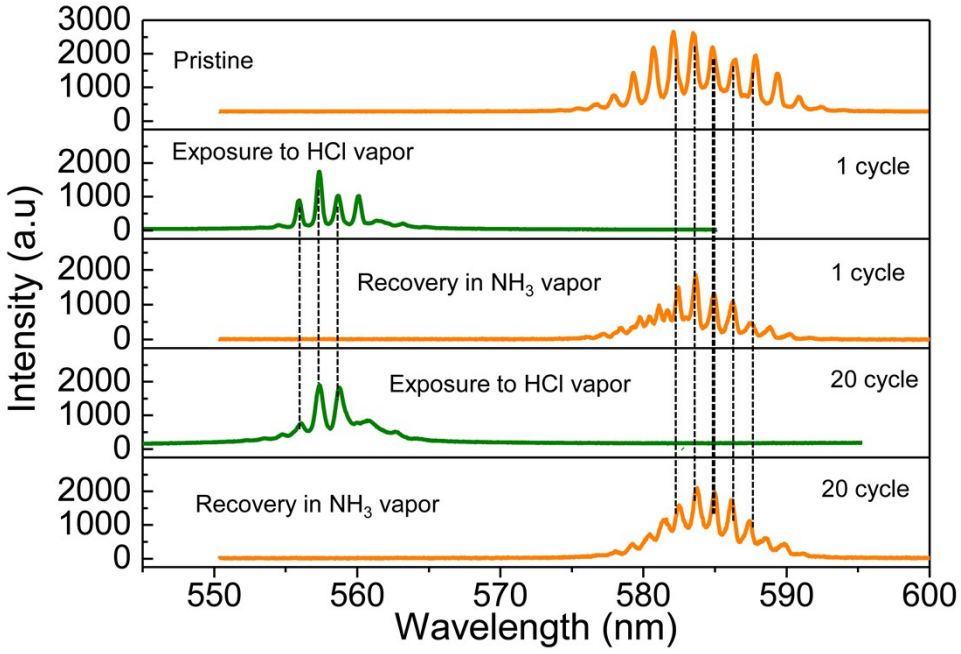

Figures S16. Microlaser emission spectra of the MBs before and after HCl–NH_3 vapor treatment.

- After introducing a small amount of N_2 gas to remove the residual HCl, adding 8 μL of NH_3 vapor accelerates the reversed chemical reaction from OPV-DMBA$^+$ • HCl$^-$ to OPV-DMBA, bringing on the lasing peaks recovering from the 560 nm to the coexistence of the two peaks of the 585 nm and the 560 nm to the single 585 nm lasing peak consistence with the initial one in 5s.
- Using the gas flowing system, the intensity and the shape of the lasing spectra would undergo changes after tens of continuous cycles. However, the lasing spectral shift

remained almost unchanged. The chemical reaction tunable switch can still work after several continuous cycles with HCl-NH_3 treatment using the gas flowing system, indicating a high stability and reliability

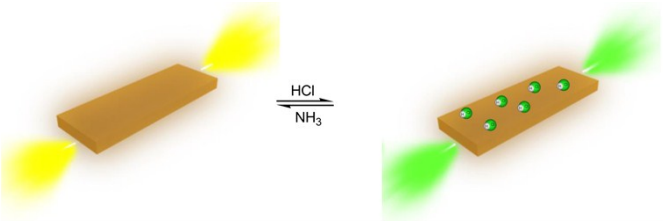

- **Figure S17.** Schematic illustration for chemical tunable and a reversible organic microcrystal laser switch.

In this work, we demonstrated a stimuli-responsive and chemically switchable organic microbelt laser through reversible protonation-deprotonation reactions. When treating with HCl-NH3 vapor cycle, the protonation−deprotonation reactions lead to a reversible microlaser switch between 585 nm (orange) and 560 nm (green) with good reproducibility and photostablity. The good reversible emission can be ascribed to the following reasons.

(ⅰ) The OPV-DMBA molecules stack in a face-to-face configuration along the crystal b-axis, leaving the dimethylamino group exposing on the surface layers of microbelts which can be protonated upon exposure to HCl vapor, forming unilayer of $DMBA^+ \cdot HCl^-$ on the surface of the microbelts through the process of chemical adsorption. When exposure to NH3 vapor, the reversed chemical reaction from $OPV\text{-}DMBA^+ \bullet HCl^-$ to OPV-DMBA happened on the surface of the microbelts.

(ⅱ) Using the Gaussian03 programs at B3LYP/6-31G** level, the energy change containing zero-point vibrational energy in OPV-DMBA + HCl -> $OPV\text{-}DMBA^+ \bullet HCl^-$ gas phase is -6.96 Kcal/mol, and the changes of Gibbs free energy is 1.97 Kcal/mol at normal temperature, which is very small. The reaction is basically reversible, which is consistence with the experiment results. Without NH_3, the lasing peaks of the MBs can be recovered from the 560 nm to the 585

nm after 24 hour, as the HCl vapor in the confocal dish evaporated in air. Moreover, with the air or the N_2 was introduced in the gas flowing system, the recovery time can be shorten to 2 minutes.

(iii) In the experiment, the solid particles of NH_4Cl haven't been observed on the surface of the microbelts:

a) We utilized a gas flowing system to realize the switchable microlaser. As schematically illustrated in Figure 3A, some OPV-DMBA microbelts was sealed in the chamber, where HCl vapor, N_2 gas and NH_3 vapor could be introduced in real time. In every experiment, a small amount of N_2 gas is introduced into the gas flowing system to remove the residual HCl vapor or NH_3 vapor. The amount of formed NH_4Cl is very little and could be taken away from the confocal dish with the gas flowing.

b) The NH_4Cl molecules begin to decompose to NH_3 and HCl gas when heated to 100 ℃. When pumped above the threshold (about 20 $\mu J \cdot cm^{-2}$), the thermal effects due to laser pumping density cause the temperature on the surface on microblets is much higher than 100 ℃. The generated NH3 and HCl gas are taken away from the confocal dish with the gas flowing.